Compact Point-of-Care Device for Self-Administered HIV Viral Load Tests from Whole Blood

Tianyi Liu[1], Anthony J. Politza[2], Aneesh Kshirsagar[1], Yusheng Zhu[3] and Weihua Guan[1, 2 *]

[1] Department of Electrical Engineering, Pennsylvania State University, University Park 16802, USA

[2] Department of Biomedical Engineering, Pennsylvania State University, University Park 16802, USA

[3]Department of Pathology and Laboratory Medicine, Pennsylvania State University, Hershey 17033, USA

* Corresponding Author, Email: wzg111@psu.edu

Abstract

HIV is a significant problem to consider, as it can lead to AIDS. Fortunately, AIDS is manageable through antiretroviral therapy (ART). However, frequent viral load monitoring is needed to monitor the effectiveness of the therapy. The current RT-PCR viral load monitoring is highly effective but is challenged by being resource-intensive and inaccessible as well as its turnaround time does not meet demand. An unmet need exists for an affordable, rapid, and user-friendly point-of-care device that could revolutionize and ensure therapeutic effectiveness, particularly in resource-limited settings. In this work, we explored a point-of-care HIV viral load device to address this need. This device can perform streamlined plasma separation, viral RNA extraction, and real-time RT-LAMP semiquantitative testing in an ultra-compact device. We developed an absorption-based membrane plasma separation method suitable for finger-prick blood samples, achieving an efficiency of 80%. We also designed a syringe-based RNA extraction method for on-site plasma processing with a viral recovery efficiency of 86%. We created a portable device with a smartphone interface for real-time semiquantitative RT-LAMP, useful for monitoring viral load. The device uses lyophilized reagents, processed with our lyophilization method, which remain stable for 16 weeks. The device can accurately categorize viral load into low, medium, and high categories with 95% accuracy. We believe this point-of-care HIV self-test device, offering convenience and long-term storage, could aid patients in home-based ART treatment monitoring.

Keyword

HIV, Viral Load, Self-Testing, Nucleic Acid Testing, RT-LAMP, Quantification

HIV remains a severe global health issue, claiming over 40.1 million lives to date, according to the World Health Organization (WHO) [1]. Nonetheless, implementing Antiretroviral Therapy (ART) has markedly mitigated morbidity and mortality in HIV-1 infected patients [2,3]. ART's main objective is the reduction of the HIV viral load (VL) to levels that are undetectable, thereby rendering the virus unable to perpetuate transmission [4,5]. In the year 2020, the Joint United Nations Program on HIV/AIDS (UNAIDS) articulated a robust 95-95-95 target: by the year 2025, 95% of all individuals affected by HIV are expected to be aware of their status; 95% of those identified should be recipients of ongoing antiretroviral therapy; and 95% of all those engaged in therapy ought to achieve viral suppression [6]. The realization of these objectives demands significant augmentations in HIV diagnostics, the assimilation of treatment, and the containment of the virus, as the curtailment of future HIV transmission intrinsically relies on these components. However, while ART can suppress viral replication, it is not a cure. Lifelong therapy is necessary due to viral persistence, residual inflammation, and metabolic disturbances, all linked to the existence of viral reservoirs [7]. These factors can lead to disease progression towards acquired immune deficiency syndrome (AIDS), even in those receiving ART. Regular viral load monitoring thus becomes indispensable for ensuring treatment success, the current practice of which is regular visits to healthcare facilities [8].

The rapid and accurate quantification of HIV viral load is critical for the effective management of HIV infection [9]. However, creating and advancing point-of-care (POC) devices for assessing HIV viral load introduces substantial and intricate challenges [10]. While highly sensitive and specific, traditional laboratory-based testing methodologies, such as reverse transcription-polymerase chain reaction (RT-PCR), are time-consuming, resource-intensive, and necessitate advanced laboratory infrastructure and trained personnel [11]. These factors often result in prolonged turnaround times for results, particularly for low-resource settings where the HIV burden is often the highest. Moreover, access to regular viral load monitoring is challenging in rural or remote regions due to the geographical distance to equipped laboratories [12]. This lack of accessibility can delay treatment adjustments and potentially accelerate disease progression [13]. Additionally, the need for venous blood sampling can be an obstacle due to the discomfort and expertise required for the procedure. Hence, a POC device for (semi)quantitative HIV viral load testing that is affordable, user-friendly, rapid, and requires minimal infrastructure could revolutionize HIV management by enabling timely and accessible monitoring, particularly in low-resource settings.

Several commercially available instruments, like the GeneXpert HIV-1 Viral Load Test (Cepheid), the Alere q system, Roche's Cobas Liat™ System, and the EOSCAPE-HIV™ HIV Rapid RNA Assay system from Wave 80 Biosciences, have been developed for HIV viral load detection. Typically, these devices utilize plasma as the specimen for testing, extracted from venipuncture whole blood within a controlled laboratory environment. As a result of this requirement, these instruments are not particularly suited for self-administered testing procedures, where more readily accessible sample types such as finger-prick whole blood would be more desirable [15–17]. In the domain of quantitative POC HIV self-testing, there have been efforts, though limited, to create and optimize systems [18]. The majority of these methodologies are dependent on complex, high-cost analyzers and opt for the use of portable thermal cyclers instead of traditional real-time PCR machinery [19].

Isothermal amplification technologies, such as reverse transcription loop-mediated isothermal amplification (RT-LAMP), have seen increased adoption in POC settings [20]. Unlike conventional PCR tests, RT-LAMP doesn't require a thermocycler. RT-LAMP maintains a comparable level of specificity and sensitivity to PCR tests [21], but provides a faster time to result and better tolerance to impurities [22]. These attributes contribute to making RT-LAMP quicker, easier to use, and more cost-effective than RT-PCR assays [23], solidifying its suitability for POC diagnostics [24]. RT-LAMP has demonstrated resilience to inhibitors in complex samples such as blood, a distinct advantage over PCR [25]. There's a growing focus on developing Nucleic Acid Testing (NAT) devices employing isothermal amplification. This innovation eliminates the need for thermal cycling and costly apparatus, marking substantial progress in the field [19,26–33]. Nevertheless, despite advances in developing these devices, significant limitations persist. At present, there exists no POC device capable of facilitating HIV viral load self-testing due to the following challenges: the inability to process whole blood samples [34], the absence of quantitative or semiquantitative capabilities within a single run [33,35–38], and the requirement for reagents to be stored at room temperature for extended periods. These pressing issues highlight the critical need for the development of an advanced HIV viral load monitoring device, one that operates from sample to answer and is suited for point-of-need usage.

In this study, we demonstrated an ultra-compact POC device with lyophilized reagents for semiquantitative self-testing of HIV viral load. Starting from 100 μL of whole blood, the device streamlines plasma separation, viral RNA extraction, and real-time RT-LAMP with built-in

internal references for semi-quantification tests. We developed an efficient membrane absorption-based plasma separation technique to overcome the challenges of the limited volume of plasma under test. We achieved 80 ± 2.3% (Hematocrit is 40%) plasma separation efficiency using this approach. We also developed a facile instrument-free syringe-based viral RNA extraction method and achieved 86 ± 1.7% (VL = 25 copies/μL) viral recovery. To facilitate the user experience, we developed a smartphone-based interface for real-time viral load monitoring. Furthermore, we also developed the lyophilized reagents in-house and demonstrated their stability at room temperature for at least 16 weeks. We assessed the performance of our device using contrived whole blood samples in conjunction with clinically obtained plasma samples. The results demonstrated an accuracy of 95% and displayed a 99% agreement with the standard benchtop RT-PCR method. These results suggested the developed device would be ideal for frequent HIV viral load self-testing at home, enhancing the monitoring of the ART treatment. We envision this device could serve as a starting point for providing rapid and easy-to-use HIV viral load self-testing solutions for the betterment of patient care.

Results and Discussion

Overall workflow

Figure 1a shows all the required materials for the whole workflow. **Figure 1b** shows the comprehensive workflow of the HIV viral load self-testing device. The workflow includes these steps: Step 1 - The user activates the app on their Android phone, which provides instructions for all subsequent steps. Step 2 - The user independently collects approximately 100 μL of blood through a finger prick, employing a disposable pipette. This blood sample is then introduced into a plasma separation card. The plasma separates from the blood cells as the blood sample passes through the card's membrane and is collected onto an absorbent paper. According to the datasheet of Vivid™ Plasma Separation GR, it is recommended to wait for 1 minute to ensure complete filtration. The now isolated plasma is readily collected for downstream analysis, serving potential applications in diagnostics, medical research, and transfusion medicine. Step 3 - The user employs disposable tweezers to detach the absorbent paper from the plasma separation card along the predefined perforated line. The absorbent paper is transferred into a collection tube preloaded with 800 μL of lysis buffer. After the transfer, the user agitates the tube to facilitate lysing and mixing.

Step 4 - Concurrently, the user assembles the RNA extraction silica column onto a 10 mL syringe within the RNA extraction module using a connector and removes the tube's transportation valve. Following a one-minute lysis period, the user utilizes a disposable pipette to transfer the solution from the lysis tube to the RNA extraction silica column. The syringe is drawn so that all the lysate within the RNA extraction silica column travels through the silica membrane and enters the syringe. The user then disconnects the lysis tube and connects tube one (packaged with two wash buffers and deionized water), drawing the syringe to allow the first two blocks to flow through the silica membrane. After completing these steps, the user switches the 10 mL syringe to a 1 mL one, draws the syringe to finalize the elution step, and stores the eluted RNA in the syringe. The connector of the syringe containing the eluted RNA is then removed, and the RNA is injected into the PCR reaction tube. Step 5 - The user inserts the test tube into the analyzer, initiating the test. Step 6 - Following 40 minutes, the APP generates and reports the final result. The entire process can be completed independently by the user at home without the need for professional personnel or laboratory equipment, enabling self-testing for HIV viral load.

Development of the lyophilized RT-LAMP assay

In the context of HIV viral load self-testing, it is imperative for the reagents to possess an excellent limit of detection (LOD), high accuracy, specificity, as well as quantitative or semiquantitative detection capacity. Furthermore, these reagents should have the capacity to be stored at room temperature for extended periods, enabling efficient transport and storage. To facilitate the development of the HIV viral load testing assay, we utilized RT-LAMP to amplify the POL (polyprotein) genes of the HIV-1 subtype B (**Figure 1c**). We validated the HIV-1 RT-LAMP primer set against the highly conserved region of the integrase gene within subtype B [39], in conjunction with a modified fluorescent reporter of Calcein [24,33]. For long-term reagent storage, we employed lyophilized reagents [40]. The pre-validated primers were added to the commercial master mix (Lyo-Ready™) to produce lyophilized RT-LAMP (**Table S1-2** provides a summary of the HIV-1 lyophilized RT-LAMP primers, the reaction setup).

To test the performance of lyophilized RT-LAMP, especially its quantitative detection capability and limit of detection, we first assessed the intrinsic copy number sensitivity of the HIV-1 lyophilized RT-LAMP assay by conducting the RT-LAMP reaction against a quantitative panel of HIV-1 RNA, at concentrations ranging from 10^5 down to 1 copy/μL. As shown in **Figure 1d-e**,

the copy number sensitivity of the lyophilized HIV-1 RT-LAMP was determined to be 16 copies (**Table S3**). Moreover, the linear fit produced an R^2 of 0.9, as fresh as when reconstituted from powder, thereby demonstrating the semiquantitative detection capacity of the HIV viral load test.

Having confirmed the functionality of our lyophilized RT-LAMP, we proceeded to examine its long-term storage performance. Two experimental configurations were prepared: one consisting of lyophilized RT-LAMP without RNA (W/O RNA), and the other including lyophilized RT-LAMP with RNA (W/ RNA, 1000 copies/rnx). The latter served as positive controls and internal references for HIV VL examination. All HIV-1 lyophilized RT-LAMP shelf-life trials were conducted at ambient temperature (23 °C), with specimens securely stored in isolated zipper bags.

During the 16-week evaluation period, the lyophilized RT-LAMP W/O RNA consistently displayed an amplification curve after introducing fresh HIV-1 RNA (1000 copies/rnx), corroborating the effectiveness of the lyophilization process (**Figure 1f**). Furthermore, the positive control, equipped with internal RNA lyophilization, also demonstrated functionality (**Figure 1g**). Both variations of the samples consistently manifested stable "time to positive" outcomes (**Figure 1h**). This consistency indicates the test's accuracy could be maintained for up to 16 weeks of storage, even with the shifts in enzymatic activities.

Plasma separation

Plasma is considered the gold standard for HIV viral load testing. Many endeavors have focused on developing plasma separation technologies from undiluted whole blood for POC applications, particularly those leveraging membrane-based plasma separation [41–50]. However, many of these technologies are complex, with low plasma separation efficiency, and challenging to operate by those without expertise or a lab environment. We have developed a straightforward, power-free plasma separation technology that employs a Vivid plasma separation membrane and an absorbent material. For materials and production processes regarding plasma separation card, please refer to the **supplementary text**. **Figure 2a** illustrates the plasma separation apparatus we devised, which primarily consists of two sections: the absorber, incorporating the absorbent membrane, and the filter, containing the Vivid plasma separation membrane. These two sections are affixed to the top and bottom covers using double-sided adhesive and are stacked together. In operation, one would drop 100 μL of blood samples, collected from the fingertip, onto the top layer of the separation card. The plasma would then flow through the filter layer and be collected in the

storage layer, while red blood cells would be retained within the filter layer. After two minutes, the top surface of the plasma separation membrane appears dry, with the absorbent material transitioning to an orange/pink hue due to plasma absorption, contrasting with its initial white color. The absorbent material can subsequently be extracted and transferred into a test tube containing lysis solution for further processing, using disposable tweezers.

First, we tested the quality of the plasma separated using our plasma separation card and compared it with the traditional laboratory protocol (We used the protocol provided by the manufacturer for QIAamp Viral RNA Kits for Total RNA). One important indicator for measuring the quality of the separated plasma is to measure the hemoglobin content in the plasma. The lower the hemoglobin content in the plasma, the higher the quality of the separation [51]. The testing blood sample volume was 100 μL, with a hematocrit of 45%. The plasma separation card utilized a separation membrane (PMS) with a diameter of 16mm. Each experimental group was repeated three times. **Figure 2b** displays the hemoglobin content measurements, which indicate that the hemoglobin content in plasma separated by our module is significantly lower than in whole blood, mirroring the efficiency of traditional centrifugal separation methods. Concurrently, microscopic imaging validates that the separated plasma is nearly devoid of red blood cells and other residues.

After confirming that the plasma separation card ensures the quality of plasma extraction, we tested the effect of the size of the plasma filtration membrane on the plasma extraction efficiency. We identified the optimal size of the plasma filtration membrane to optimize extraction efficiency. The plasma extraction efficiency of our plasma separation card relies mainly on the size of the plasma filtration membrane [45]. A small membrane may become rapidly clogged by the red blood cells in whole blood, thereby halting filtration. Conversely, an overly large membrane may retain a non-permeable “dead volume” of remaining plasma that the absorbent material cannot capture. In the context of HIV viral load self-testing, we sought to extract 100 μL of whole blood from fingertip samples, utilizing five different diameters of plasma filtration membranes, ranging from 12 to 20 mm. By measuring the plasma paper weight change before and after the absorbing process, we estimated the plasma extraction efficiency. We maintained the diameter of the absorbent material at 16 mm as the initial filtered blood volume was established at 100 μL, and a 16 mm diameter absorbent material can sufficiently absorb 100 μL of plasma. Notably, in a given 100 μL sample of whole blood, the plasma volume commonly represents a maximum proportion of roughly 60 μL. As depicted in **Figure 2c**, the 16 mm diameter filter membrane yields an efficiency

of about 80%. Importantly, this extraction is less affected by varying hematocrit levels when using the 16 mm diameter filter membrane. Our developed plasma separation card achieves an extraction efficiency of 80% while ensuring the quality of the extracted plasma. It is user-friendly, cost-effective, and suitable for self-testing applications for HIV viral load tests.

Syringe-based RNA extraction module

One of the essential steps in HIV viral load testing is the extraction of RNA from the sample (plasma). The method of solid-phase extraction, employing a silica membrane to engage with RNA alongside chaotropic salts, offers a streamlined alternative for RNA's swift isolation. This approach is facilitated within a singular tube and stands as a comparatively uncomplicated process, applicable for self-testing of HIV viral load [52,53]. A variety of commercial kits, produced and distributed by several enterprises, are accessible for this purpose. The underlying mechanism involves RNA affixed to silica membranes through chaotropic salts, forming salt bridges. Following multiple wash phases, the RNA is eluted by adjusting the saline concentration [54]. Though this process is both uncomplicated and practical, every stage necessitates centrifugation, an element that may not be practical for in-field applications, particularly within environments constrained by resources [55]. In response to these challenges, our work has paved the path of a centrifugation-independent, syringe-structured viral RNA extraction module for HIV viral load self-testing, thereby enhancing user accessibility.

Figure 3a depicts the conceptual design of a syringe-driven RNA extraction module, consisting of three essential elements and its underlying operating mechanism: (i) a silica membrane filter specifically engineered to adhere to RNA molecules under conditions of elevated salt concentration; (ii) flexible tubing employed to contain the wash and elution buffers, delineated by a custom-crafted manual valve that isolates each successive portion of the reagent. (iii) Two syringes are used to create negative pressure, allowing the reagent in the soft tubes to flow through the silica membrane filter. For materials and production processes regarding Syringe-based RNA extraction module, please refer to the **supplementary text**. One syringe is used to collect the washing buffer, while the other is used to collect the eluted RNA. The absorbent part of the plasma separation card is placed into a lysis tube for sample lysis, releasing RNA into the lysis solution. The lysis tube is connected to the silica membrane and a syringe. By drawing and pushing the syringe, all the solutions flow through the silica membrane, allowing the RNA to bind to the

membrane. The valve on the storage buffer reagent tube is released and connected to the silica membrane, replacing the lysis tube. By pulling the syringe, the first two segments of the solution from the storage buffer reagent tube pass through the silica membrane, completing the washing procedure. The syringe is then replaced with a 1-milliliter syringe, and by pulling the syringe again, the last segment of the solution (DI water) from the storage buffer reagent tube flows through the silica membrane and is drawn into the syringe, completing the elution procedure.

In order to test the RNA recovery rate of the Syringe-based RNA extraction module, we prepared mock plasma samples of varying concentrations by mixing different amounts of virus particles into commercial plasma. Each mock plasma sample had a volume of 40 μL, simulating the approximate volume extractable from 100 μL of whole blood using the plasma separation card. The sample concentrations ranged from 500 to 25,000 copies/ml of plasma, covering the typical range of viral loads found in HIV patients. We extracted RNA from the mock plasma samples using our syringe-based RNA extraction module and performed quantitative analysis using RT-qPCR. The real-time HIV-1 RT-qPCR amplification curve can be found in (**Figure S1a&b**). We establish a reference line using PCR reactions with known copy numbers. Given the excellent quantification capabilities of PCR (with a linear fit R^2 of 0.99), we can calculate the quantity of RNA in unknown samples by comparing their measured Cq values to the reference line. **Figure 3b** shows RT-PCR fitted reference lines were generated to quantify the copy numbers of extracted RNA. The black squares indicate the reference reaction with known copy numbers. The blue dots represent RNA extracted using the lab-based protocol, while the red dots represent RNA extracted using the syringe-based method. These values are calculated averages obtained from three repeated experiments. By using the known viral load and solvent of the mock plasma samples, along with the RNA copy number extracted through PCR Cq values and the reference line, we can calculate the RNA extraction efficiency of the syringe-based RNA extraction module (**Figure S1c&d**).

Figure 3c shows RNA extraction efficiency for different concentrations by using our syringe-based RNA extraction module compared with the lab-based protocol (centrifugation). From the figure, we can see that although our syringe-based RNA extraction module efficiency is lower than the laboratory protocol, we can still recover the major RNA which lab-based protocol can recover. For high-concentration samples (VL ~ 25000 copies/ml), our extraction module can reach about 95% of the extraction efficiency. For low-concentration samples (VL ~ 1000 copies/ml), our extraction module can reach about 40% of the extraction efficiency. For the standard protocols of

our extraction module and laboratory, the extraction efficiency decreases accordingly when the sample concentration is reduced. One probable reason is that the silicon filter has dead volume and part of the RNA is caught and cannot be extracted. Based on existing data, it can prove that our RNA extraction module can complete the RNA extraction without using power, which is suitable for field testing or self-testing.

Analyzer development and analytical evaluation

Next, we developed a prototype portable analyzer capable of performing RT-LAMP assay amplification and quantifying the resultant fluorescent output. **Figure 4a** illustrates the disassembled and assembled views of the analyzer. This compact device features an internal Li-Ion battery and Bluetooth connectivity, integrating electronic, optical, and thermal subsystems into an ultra-portable form factor. Based on the NAT-On-USB device [33], we've updated our analyzer with an optical module featuring three distinct excitation and detection units for real-time fluorescence monitoring. For materials and production processes regarding analyzer, please refer to the **supplementary text**. We reduced excitation interference by arranging the units perpendicularly. The 555 nm channel was chosen for Calcein detection due to its low interference and optimal responsiveness, and normalization based on the 480 nm channel minimized potential signal errors. The module displayed a strong linear correlation ($R^2 = 0.94$) between the relative fluorescence unit and Calcein concentration (**Figure S2**). Our thermal module, integrating a power resistor, a thermistor, and an insulated housing, achieves the required 60 ℃ within 3 minutes with a stable temperature of 0.074 ℃ RMS value, meeting the LAMP assay requirements. With the inclusion of thermal insulation made of 3D-printed ABS material and foam sealant, energy consumption during the heating and incubation stages is reduced by about 22%, and the power resistor's duty ratio is effectively decreased (**Figure S3**). Our analyzer employs custom circuit boards for temperature and fluorescence management powered by a replaceable lithium-ion battery. Test results are accessible via a Bluetooth-enabled mobile app with a custom GUI.

In our quest to assess the quantitative detection performance of our newly designed analyzer, we tested serially diluted HIV-1 RNA samples. With these samples, we undertook the amplification process utilizing our reconstituted lyophilized RT-LAMP. The analyzer's performance was monitored through a panel of these samples tested in triplicate. The real-time data from these tests (**Figure 4b**) demonstrated that our analyzer successfully amplified HIV-1

RNA at a concentration of 25 copies per reaction. In addition, the time to positive as a function of the input RNA concentrations (**Figure 4c**) shows a clear linear relationship ($R^2 = 0.9$), which suggests the analyzer's practical applicability in semiquantitative clinical sample testing.

Diagnostic performance from sample to answer

To illustrate the clinical utility of our HIV self-test device, we examined 20 archived clinical HIV samples sourced from Penn State Hershey Medical Center's HIV/AIDS outpatient clinics. These samples contain 10 HIV-positive patients with three levels of viral load (VL) (Low: 0 - 1,000; Medium: 1,000 - 20,000; High: > 20,000 copies/mL) [56,57], along with 10 HIV-negative individuals confirmed by Roche COBAS® AmpliPrep. To compare the HIV self-test device with RT-PCR, we tested two identical samples using each method.

To evaluate our device's performance agreement with benchtop PCR, we also extracted RNA using the traditional centrifugation method and performed PCR testing on these samples. Both the RT-PCR process and the HIV self-test device used an identical volume of 25 μL for analysis, with the former employing a column-based extraction method. **Figure 5a** displays the real-time RT-PCR results of these clinical samples alongside six concentration references for quantification, with the RT-PCR calibration curve illustrated in **Figure S4**. **Figure 5b** presents the data obtained through RT-LAMP analysis from our HIV self-test device, encompassing a set of 20 clinical specimens, inclusive of both positive and negative results. For each test, there are two internal references (lyophilized RT-LAMP reagents with known RNA concentrations). These internal references facilitate the differentiation between three levels of viral load.

Figure 5c provides a qualitative and semiquantitative analysis using PCR and our device. The green boxes signify clinical samples without HIV infection or from individuals receiving antiretroviral therapy (ART) with a successfully suppressed viral load within a safe range. The orange boxes denote clinical samples with a viral load surpassing the safe range, signaling a necessity for further medical monitoring. The red boxes illustrate samples with a higher viral load, indicative of treatment failure and viral rebound despite ART. By employing Cq values of 33 and 26, we can classify the viral load into three distinct levels. The inset table summarizes the qualitative test results using a 40-minute threshold to determine outcomes in our semiquantitative test. Our analyzer adopts a comparative internal reference method to yield final output results: Low, Medium, and High. The calculated accuracy is 95%, suggesting the ability of our test to

categorize viral load into Low, Medium, and High categories.

For the device's quantitative viral load analysis capabilities, we compared the time to positive from our device with the Cq from benchtop PCR. **Figure 5d** displays a scatter plot that represents the correlation between the mean Cq values of RT-PCR results and the Time-To-Positive measured by the analyzer, which showed a strong Pearson correlation of $r = 0.99$. This indicates excellent agreement between our device and the benchtop PCR instrument. With an accuracy of 95%, we demonstrate that our device is capable of performing semiquantitative HIV viral load tests and that it can inspire confidence for the implementation of the proposed point-of-care platform in areas where HIV viral load tests are necessary.

Conclusion

In summary, we demonstrated the potential of a point-of-care HIV viral load self-testing device engineered to address current diagnostic challenges, particularly in low-resource settings. Our device, requiring 100 µL of finger-prick blood, offers a convenient, efficient, and non-invasive testing alternative, reducing the need for venous blood samples. With the integration of a smartphone interface, our tool provides real-time semiquantitative HIV viral load monitoring, achieving an accuracy of 95%. In overcoming common challenges associated with existing point-of-care tests, such as the need for complex laboratory infrastructure and accessibility issues, we successfully developed efficient absorption-based plasma separation methods that achieve an efficiency of $80 \pm 2.3\%$ (hematocrit is 40%), and our syringe-based RNA extraction method for on-site plasma processing yields a viral recovery efficiency of $86 \pm 1.7\%$ (VL = 25 copies/µL). These high-efficiency rates significantly enhance the robustness of the testing process. Additionally, we incorporated the use of lyophilized reagents, enhancing the longevity and practicality of our device. Furthermore, the results of our study underscore the importance and potential of using our device for regular self-monitoring of HIV viral load, thereby supporting effective management of antiretroviral therapy. We evaluated our device using clinical samples, achieving a 95% accuracy rate and 99% agreement with conventional RT-PCR methods. These findings suggest the device's potential for routine HIV viral load self-testing at home, enhancing ART treatment monitoring. This development may be a foundational step towards more user-friendly HIV self-testing solutions to improve patient care. Future work will focus on improving device efficiency, exploring ways to lower manufacturing costs, and conducting extensive field

trials in various settings. As we move forward, we remain optimistic that our device will have implications for global health by providing a rapid, affordable, and easy-to-use solution to HIV viral load testing.

Materials and methods

Materials and Chemicals

Components for this study were sourced from various suppliers. Vivid™ Plasma Separation GR was from Pall Corp. RNA extraction materials came from McMaster (**Supplementary Table S5**), while most electronic and optical parts for the HIV analyzer were from DigiKey (**Supplementary Table S6**). RT-LAMP and RT-PCR primers were by IDT. Essential mixes and chemicals were from Meridian Life Science, Sigma-Aldrich, and ThermoFisher. The Bio-Rad CFX96 was used for assay validation. HIV-1 RNAs were from SeraCare, while blood samples were from Innovative Research. Clinical HIV samples were sourced from Penn State Hershey Medical Center. All materials were used as received and stored following manufacturer guidelines.

HIV-1 lyophilized RT-LAMP assay reaction

The RT-LAMP assay reaction, optimized for the detection of HIV-1, is detailed in **Supplementary Table S1**. This assay involves a reaction mix with a total volume of 25 µL, composed of several critical components. This mix contains an isothermal buffer, which includes Tris-HCl, $(NH_4)_2SO_4$, KCl, $MgSO_4$, Tween 20, and dNTPs, along with Bst, PCR grade H_2O and $MgSO_4$ (7 mM) were also included in the reaction mixture. Additionally, the RNA template was integrated in conjunction with a specifically designated collection of primers, consisting of 0.2 µM of F3 and B3, 1.6 µM of FIP and BIP, as well as 0.8 µM of LPF and LPB. The reaction was performed at a controlled temperature of 60 ℃ for a duration of 45 minutes. In this assay, we utilized our pre-validated primers, listed in **Supplementary Table S2**. These primers were added to the commercial master mix. The resulting samples were then frozen at -80 ℃ for 12 hours to stabilize them. After this freezing step, the samples underwent lyophilization at -50 ℃ and 0.02 mbar using a freeze-dryer from LabCon Co. This process rendered the samples stable and ready for subsequent analyses.

HIV-1 RT-PCR reaction

In the study, a two-enzyme, single-step RT-PCR technique was implemented for conducting HIV-1 examinations. The procedure involved a total reaction volume of 20 µL, comprising 5 µL of TaqMan Fast Virus 1-Step Master Mix, along with forward and reverse primers (each at 0.6 µM concentration), a probe (0.25 µM), 1 µL of RNA templates, and 11 µL of water that meets PCR-grade standards. A previously authenticated set of HIV-1 RT-PCR primers was utilized in this investigation [58]. The RT-PCR process was carried out with specific thermal cycling patterns, initiating at 50 ℃ for an initial five-minute duration for the singular non-repeating reverse transcription phase, converting HIV-1 RNA into complementary DNA (cDNA). This was succeeded by a 95 ℃ phase for 20 seconds without repetition to commence the amplification process, followed by a series of 40 amplification cycles. Each cycle involved a three-second heating at 95 ℃ and a thirty-second thermal cycling at 60 ℃. The primers used in the investigation were Forward (5'-CATGTTTTCAGCATTATCAGAAGGA-3') and Reverse (5'-TGCTTGATGTCCCCCCACT-3') at 600 nM, along with a Probe (5'FAM-CCACCCCACAAGATTTAAACACCATGCTAA-Q 3') at 250 nM. In this context, FAM refers to the reporter 6-carboxyfluorescein group, while Q symbolizes the 6-carboxytetramethylrhodamine group that functions as a quencher and is conjugated through a linker arm nucleotide.

Whole blood HIV sample

We created a whole-blood HIV sample by integrating a known concentration of HIV-1 clinical plasma sample with healthy whole blood. The process involved several stages. Initially, we centrifuged clinical whole blood samples at 1000 rpm for 10 minutes, separating plasma and red blood cells and storing them separately. We then combined 6 ml of clinical plasma with 4 ml of red blood cells, mixing and vertexing to obtain a 10 ml blood sample with an estimated hematocrit ratio of 40%. An EKF Diagnostics Hemo Control analyzer was used to confirm this ratio. Notably, our method omitted the use of Proteinase K to deactivate RNases in the whole blood, streamlining sample preparation. Unless specified otherwise, the volume of whole blood sample used in our study was 100 µL.

Statistical analysis

All statistical analysis and regression modeling were performed using MATLAB R2020 (Natick, MA). All plots displaying data represent the mean and 3 standard deviations from triplicate testing unless stated otherwise. MATLAB was used for all data processing. All figures and plots were generated using MATLAB and PowerPoint.

Author contributions

T.L. and A.K. were responsible for the design and integration of the device, while T.L. took the lead in developing and validating the RT-PCR assay. The sample preparation protocol was a collaborative effort between T.L. and A.J.P., and T.L. specifically handled the validation of the module. W. Guan initiated the concept and provided overall supervision for the study. All the authors contributed to data analysis and jointly wrote the manuscript.

Conflicts of interest

A provisional patent related to the technology described herein is filed.

Acknowledgment

This study received support from the National Institutes of Health (R61AI147419) and the National Science Foundation (1912410 & 1902503). The opinions, findings, conclusions, or recommendations expressed in this work are solely those of the authors and do not necessarily represent the views of the National Science Foundation or the National Institutes of Health.

Figures and Captions

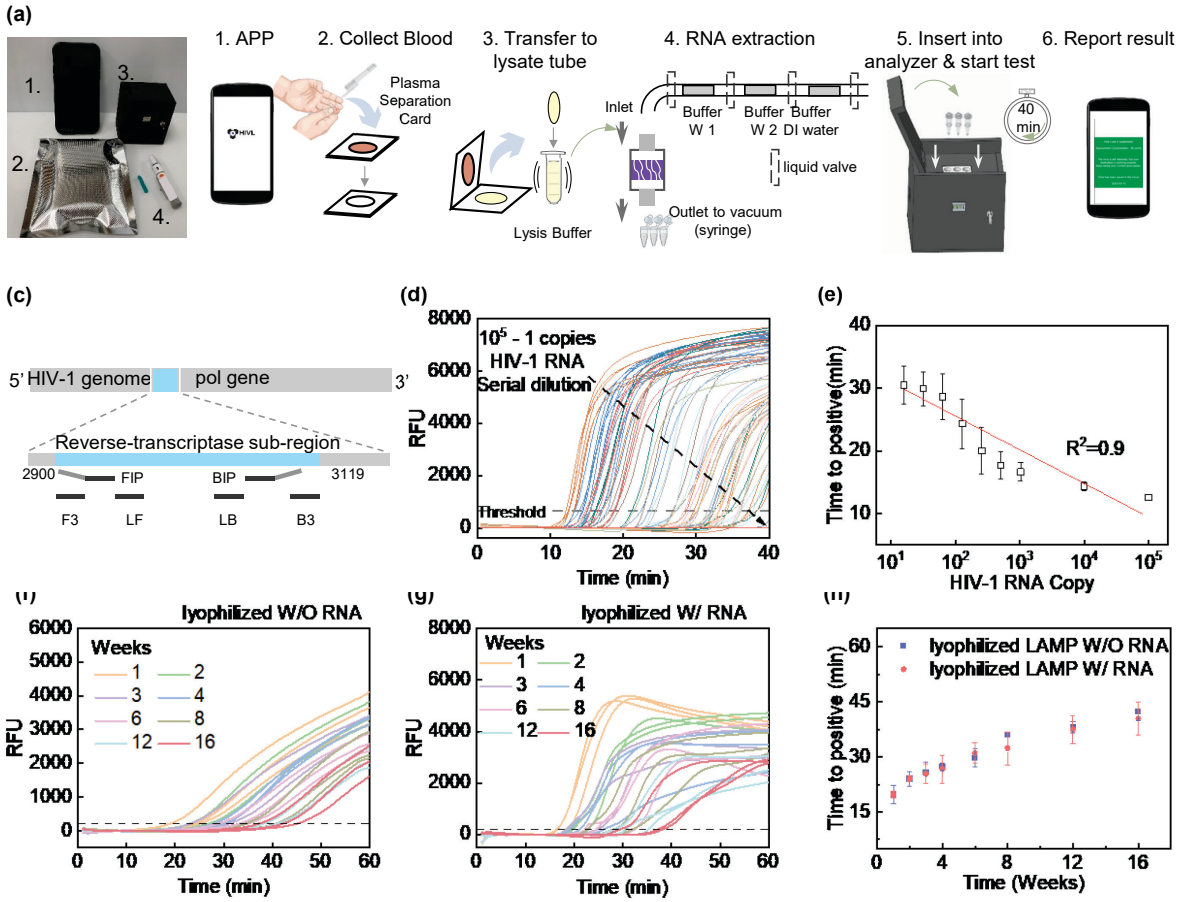

Figure 1. Overall Device Workflow and Assay Design. **(a)** An image showing the components of the device, including 1. an Android phone, 2. a syringe-based RNA extraction module, 3. an analyzer, and 4. a lancet. **(b)** The procedure, as comprehensively delineated in the mobile application, involves a user initiating the app, self-collecting a blood sample using a disposable pipette and plasma separation card, transferring the absorbent paper into a pre-filled lysis buffer collection tube, conducting RNA extraction, introducing the eluted RNA and water into the testing tube, and finally, after 40 minutes, receiving the test results via the APP. **(c)** The design of primers. This includes a set of 6 RT-LAMP primers that target the medium region of the pol gene. **(d)** Real-time HIV-1 lyophilized RT-LAMP amplification data preserved when reconstituted from powder with serially diluted HIV RNA standards (six repeats per concentration). **(e)** Duration to positive value at various HIV-1 RNA concentrations; defined as the time for the RFU to hit a 1000 threshold (dashed line in d). **(f)** Results of HIV-1 lyophilized RT-LAMP real-time amplification over 16 weeks, replicated three times weekly using PCR-grade water and lyophilized RT-LAMP powder, plus 1000 HIV-1 RNA copies. **(g)** Data showing HIV-1 lyophilized RT-LAMP real-time amplification performance within a 16-week period. Each reaction was replicated three times per testing week using only PCR-grade water and lyophilized RT-LAMP powder (containing 1000 copies of HIV-1 RNA) mixed together. **(h)** The results of a test evaluating the shelf-life of lyophilized HIV-1 RT-LAMP.

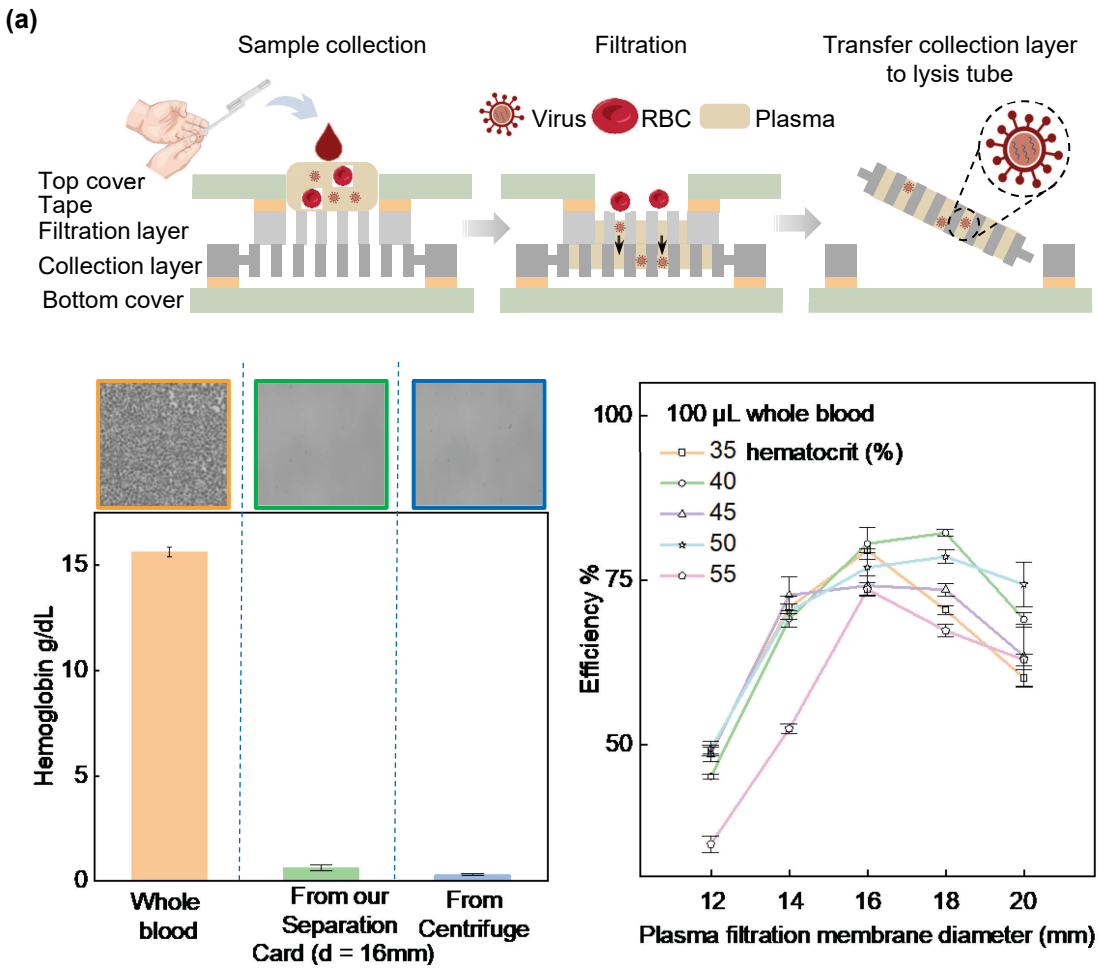

Figure 2. Schematic diagram showing its working principle and characterization of the plasma separation card **(a)** Schematic diagram showing its working principle of the plasma separation module. The plasma separation card is divided into six layers. When in use, drop 100 µL of blood samples collected by fingertips into the upper layer of the separation card. The plasma will flow through the filter layer and be stored in the collection layer, while the red blood cells will be trapped in the filter layer. **(b)** The quality (hemoglobin content) difference between plasma separated by a plasma separation card and plasma separated by the laboratory conventional method (centrifugation) was compared. The blood sample volume for testing was 100 µL, with a hematocrit of 45%. The separation membrane (PMS) diameter in the plasma separation card used was 16mm. Each experimental group was repeated three times. **(c)** The variation in the separation efficiency of the plasma separation card, as a function of hematocrit and the diameter of the separation membrane (PMS) in the plasma separation card. The volume of the tested blood sample was 100 µL, and each experimental group was repeated three times.

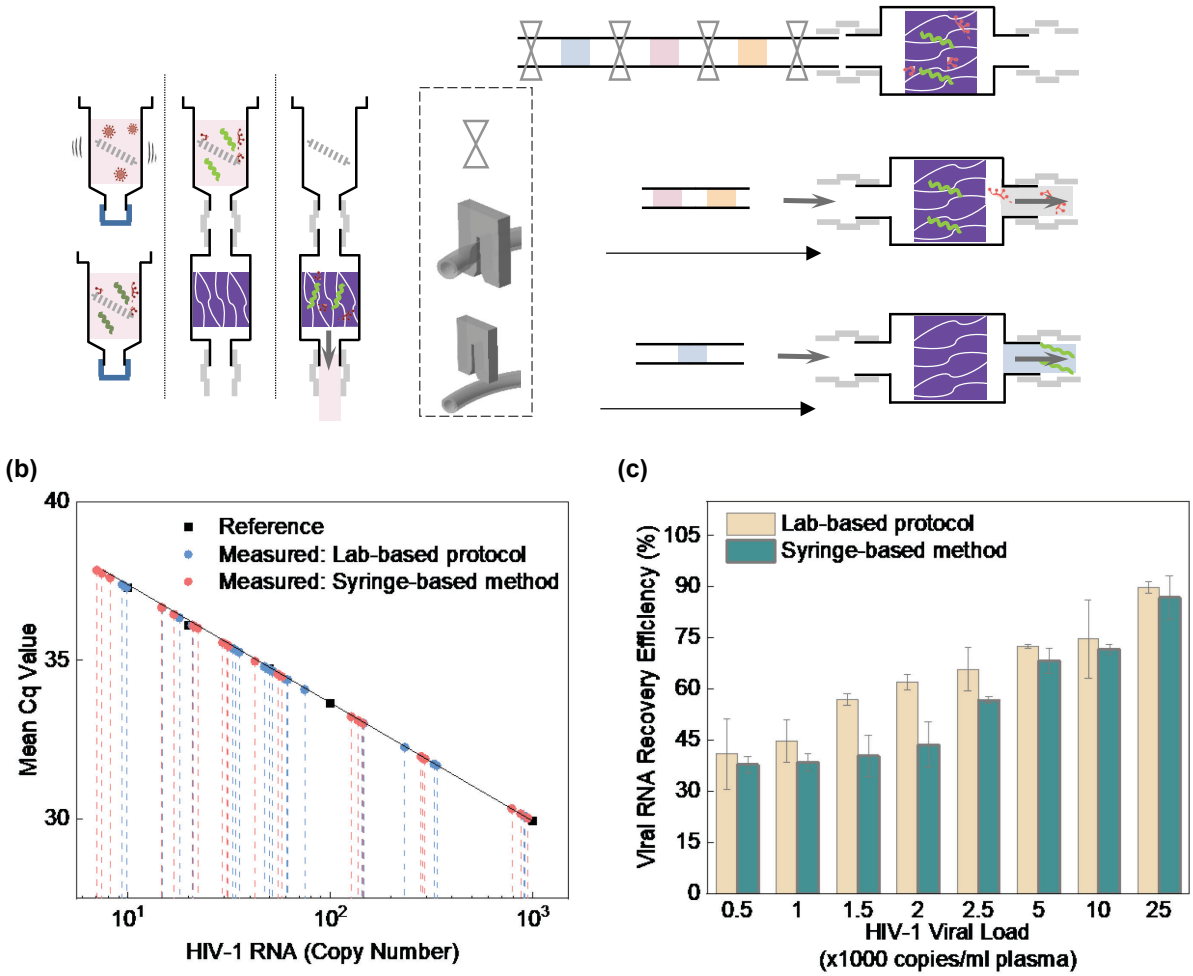

Figure 3. Schematic diagram illustrating the working principle and characterization of the syringe-based RNA extraction module. **(a)** Schematic diagram illustrating the working principle of the syringe-based RNA extraction module. The absorbent part is placed in a lysis tube for sample lysis, releasing RNA into the solution. The lysis tube is connected to the silica membrane filter using an injector. Solutions flow through the membrane, binding RNA to it. The storage buffer reagent tube replaces the lysis tube, and the first two segments of its solution flow through the membrane for washing. The last segment (DI water) is flowed through the membrane and drawn into the injector for elution. **(b)** RT-PCR fitted reference line was generated to quantify the copy numbers of extracted RNA. The black squares indicate the reference reaction with known copy numbers. The blue dots represent RNA extracted using the lab-based protocol, while the red dots represent RNA extracted using the syringe-based method. These values are calculated averages obtained from three repeated experiments. **(c)** Comparison of RNA extraction efficiency for plasma samples with varying viral loads between our extraction module and the lab-based protocol. Each group experiment was repeated three times.

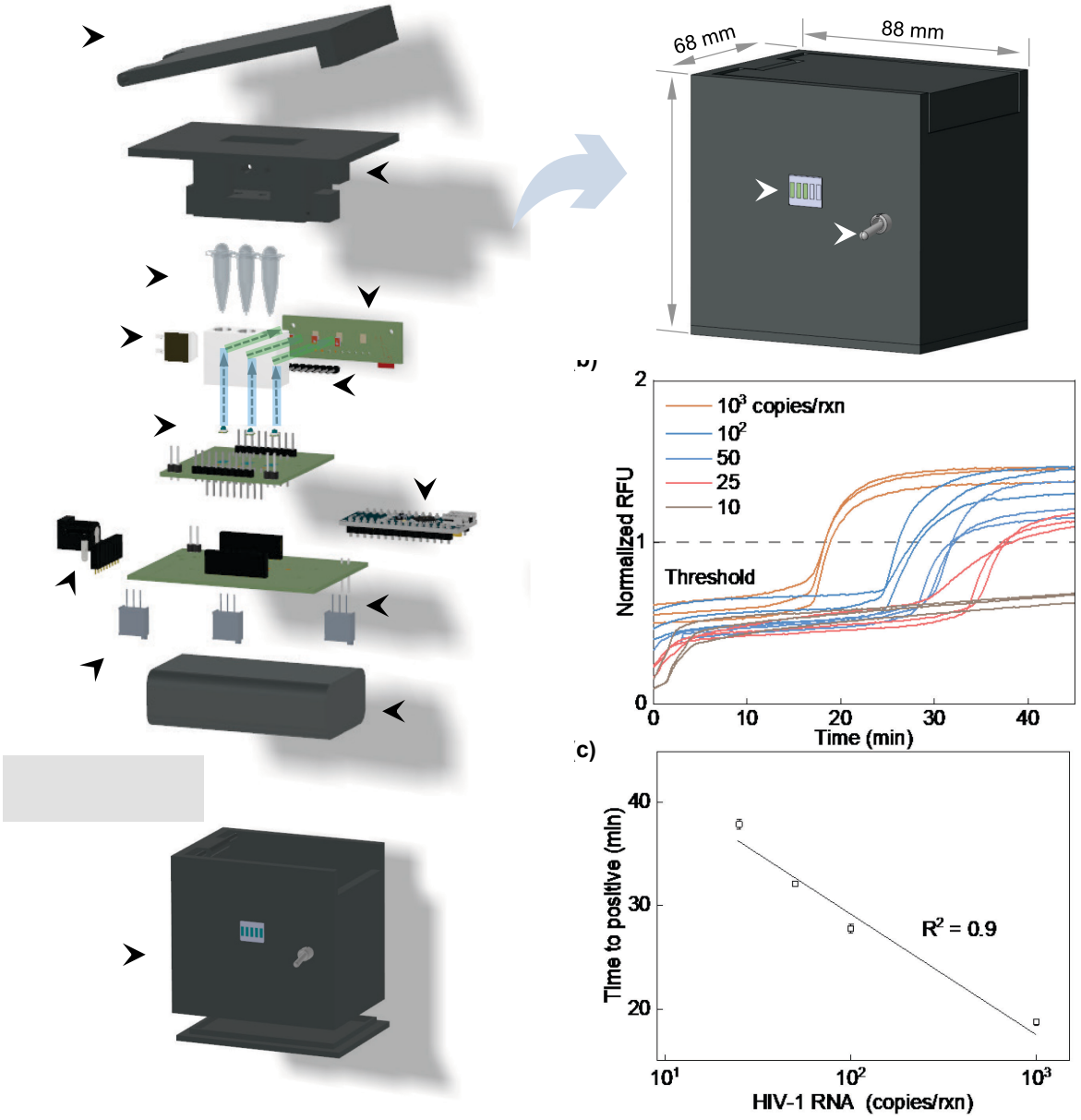

Figure 4. The analyzer and its performance for RT-LAMP amplification and detection for HIV semiquantitative self-testing. **(a)** Renderings showcase a fully enclosed analyzer along with a partially exploded view (dimensions: 88×68×82 mm; weight: 200 g). (1) Users activate the analyzer and initiate detection reactions via push buttons, with real-time updates provided by the status indicator. (2) The analyzer is Bluetooth-enabled for data transmission. Optical, thermal, and electromagnetic array subsystems are seamlessly integrated, supporting streamlined nucleic acid testing. The entire analyzer can be powered by an internally rechargeable battery. **(b)** This panel presents real-time RT-LAMP data from a single-analyzer test with serially diluted HIV-1 RNA. Each concentration was tested in triplicate. **(c)** This panel depicts the extracted "Time to positive" value from the single-analyzer test.

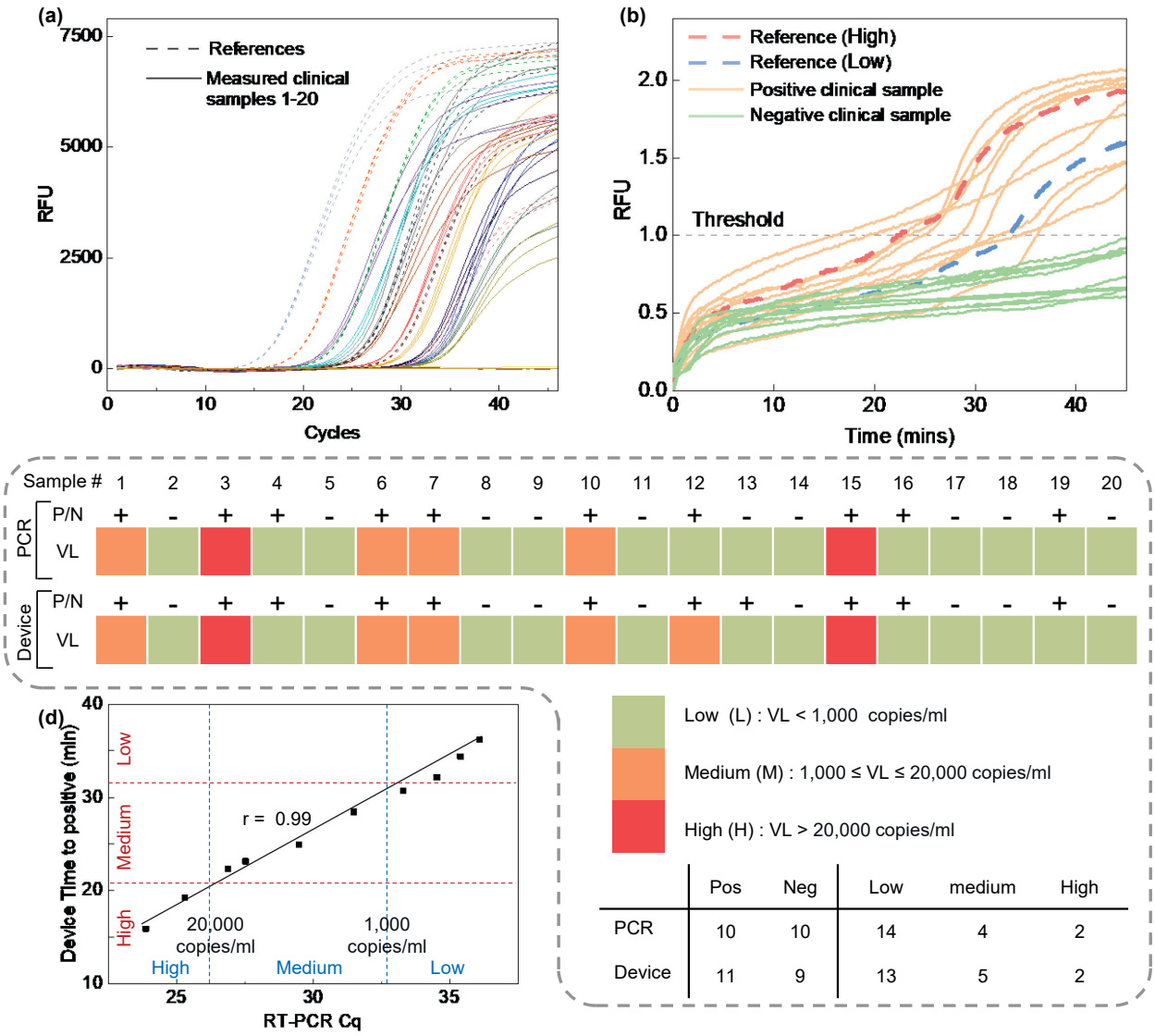

	Pos	Neg	Low	medium	High
PCR	10	10	14	4	2
Device	11	9	13	5	2

Figure 5. Testing of clinical samples using our device. **(a)** Real-time RT-PCR results for the clinical sample compared with calibration references. **(b)** Real-time RT-LAMP results were obtained from a single-analyzer test, utilizing both positive and negative clinical samples. The results were obtained using a 25 µL eluted RNA from 100 µL clinical samples. The total reaction mixture is 25 µL. **(c)** Validation using clinical samples in a blinded test. Clinical samples from 20 patients (10 negatives and 10 positives). We conducted qualitative and semiquantitative analyses using PCR and our device, respectively. **(d)** Scatter plot and the linear fitted line comparing the mean Cq values of RT-PCR results with Time-To-Positive measured by the analyzer (10 positives).

Reference

(1) *WHO. HIV Key facts*. https://www.who.int/news-room/fact-sheets/detail/hiv-aids (accessed 2023-07-05).

(2) Trickey, A.; May, M. T.; Vehreschild, J.-J.; Obel, N.; Gill, M. J.; Crane, H. M.; Boesecke, C.; Patterson, S.; Grabar, S.; Cazanave, C.; Cavassini, M.; Shepherd, L.; Monforte, A. d'Arminio; Sighem, A. van; Saag, M.; Lampe, F.; Hernando, V.; Montero, M.; Zangerle, R.; Justice, A. C.; Sterling, T.; Ingle, S. M.; Sterne, J. A. C. Survival of HIV-Positive Patients Starting Antiretroviral Therapy between 1996 and 2013: A Collaborative Analysis of Cohort Studies. *The Lancet HIV* **2017**, *4* (8), e349–e356. https://doi.org/10.1016/S2352-3018(17)30066-8.

(3) Sterne, J. A.; Hernán, M. A.; Ledergerber, B.; Tilling, K.; Weber, R.; Sendi, P.; Rickenbach, M.; Robins, J. M.; Egger, M.; Study, S. H. C. Long-Term Effectiveness of Potent Antiretroviral Therapy in Preventing AIDS and Death: A Prospective Cohort Study. *The Lancet*, 2005, *366*, 378–384.

(4) Drain, P. K.; Dorward, J.; Bender, A.; Lillis, L.; Marinucci, F.; Sacks, J.; Bershteyn, A.; Boyle, D. S.; Posner, J. D.; Garrett, N. Point-of-Care HIV Viral Load Testing: An Essential Tool for a Sustainable Global HIV/AIDS Response. *Clin Microbiol Rev* **2019**, *32* (3), e00097-18. https://doi.org/10.1128/CMR.00097-18.

(5) Hossain, M. M.; Sultana, A.; Mazumder, H. Munzur-E-Murshid. *Sexually transmitted infections among Rohingya refugees in Bangladesh. lancet HIV*, 2018, *5*, e342.

(6) Ehrenkranz, P.; Rosen, S.; Boulle, A.; Eaton, J. W.; Ford, N.; Fox, M. P.; Grimsrud, A.; Rice, B. D.; Sikazwe, I.; Holmes, C. B. The Revolving Door of HIV Care: Revising the Service Delivery Cascade to Achieve the UNAIDS 95-95-95 Goals. *PLOS Medicine* **2021**, *18* (5), e1003651. https://doi.org/10.1371/journal.pmed.1003651.

(7) Schank, M.; Zhao, J.; Moorman, J. P.; Yao, Z. Q. The Impact of HIV-and ART-Induced Mitochondrial Dysfunction in Cellular Senescence and Aging. *Cells*, 2021, *10*, 174.

(8) Phillips, A.; Shroufi, A.; Vojnov, L.; Cohn, J.; Roberts, T.; Ellman, T. Working Group on Modelling of Antiretroviral Therapy Monitoring Strategies in Sub-Saharan Africa. Sustainable HIV Treatment in Africa through Viral-Load-Informed Differentiated Care. *Nature*, 2015, *528*, S68-76.

(9) Roberts, T.; Cohn, J.; Bonner, K.; Hargreaves, S. Scale-up of Routine Viral Load Testing in Resource-Poor Settings: Current and Future Implementation Challenges: Table 1. *Clin Infect Dis.* **2016**, *62* (8), 1043–1048. https://doi.org/10.1093/cid/ciw001.

(10) Drain, P. K.; Hyle, E. P.; Noubary, F.; Freedberg, K. A.; Wilson, D.; Bishai, W. R.; Rodriguez, W.; Bassett, I. V. Diagnostic Point-of-Care Tests in Resource-Limited Settings. *The Lancet Infectious Diseases* **2014**, *14* (3), 239–249. https://doi.org/10.1016/S1473-3099(13)70250-0.

(11) Jani, I. V.; Sitoe, N. E.; Alfai, E. R.; Chongo, P. L.; Quevedo, J. I.; Rocha, B. M.; Lehe, J. D.; Peter, T. F. Effect of Point-of-Care CD4 Cell Count Tests on Retention of Patients and Rates of Antiretroviral Therapy Initiation in Primary Health Clinics: An Observational Cohort Study. *The Lancet* **2011**, *378* (9802), 1572–1579. https://doi.org/10.1016/S0140-6736(11)61052-0.

(12) Mnyani, C. N.; McIntyre, J. A.; Myer, L. The Reliability of Point-of-Care CD4 Testing in Identifying HIV-Infected Pregnant Women Eligible for Antiretroviral Therapy. *JAIDS Journal of Acquired Immune Deficiency Syndromes* **2012**, *60* (3), 260–264. https://doi.org/10.1097/QAI.0b013e318256b651.

(13) Phillips, A. N.; Cambiano, V.; Nakagawa, F.; Ford, D.; Apollo, T.; Murungu, J.; Rousseau, C.; Garnett, G.; Ehrenkranz, P.; Bansi-Matharu, L.; Vojnov, L.; Katz, Z.; Peeling, R.; Revill, P. Point-of-Care Viral Load Testing for Sub-Saharan Africa: Informing a Target Product Profile. *Open Forum Infectious Diseases* **2016**, *3* (3), ofw161. https://doi.org/10.1093/ofid/ofw161.
(14) Mazzola, L.; Pérez-Casas, C. HIV/AIDS Diagnostics Technology Landscape 5th Edition. *UNITAID*, 2015, 66–68.
(15) Fidler, S.; Lewis, H.; Meyerowitz, J.; Kuldanek, K.; Thornhill, J.; Muir, D.; Bonnissent, A.; Timson, G.; Frater, J. A Pilot Evaluation of Whole Blood Finger-Prick Sampling for Point-of-Care HIV Viral Load Measurement: The UNICORN Study. *Sci Rep-Uk* **2017**, *7* (1), 13658. https://doi.org/10.1038/s41598-017-13287-2.
(16) Bertagnolio, S.; Parkin, N. T.; Jordan, M.; Brooke, J.; Garcia-Lerma, J. G. Dried Blood Spots for HIV-1 Drug Resistance and Viral Load Testing. *Aids Reviews* **2010**, *12* (4), 195–208.
(17) Guichet, E.; Serrano, L.; Laurent, C.; Eymard-Duvernay, S.; Kuaban, C.; Vidal, L.; Delaporte, E.; Ngole, E. M.; Ayouba, A.; Peeters, M. Comparison of Different Nucleic Acid Preparation Methods to Improve Specific HIV-1 RNA Isolation for Viral Load Testing on Dried Blood Spots. *J Virol Methods* **2018**, *251*, 75–79. https://doi.org/10.1016/j.jviromet.2017.10.014.
(18) Ngo, H. T.; Jin, M.; Trick, A. Y.; Chen, F.-E.; Chen, L.; Hsieh, K.; Wang, T.-H. Sensitive and Quantitative Point-of-Care HIV Viral Load Quantification from Blood Using a Power-Free Plasma Separation and Portable Magnetofluidic Polymerase Chain Reaction Instrument. *Anal. Chem.* **2022**, acs.analchem.2c03897. https://doi.org/10.1021/acs.analchem.2c03897.
(19) Mauk, M.; Song, J.; Bau, H. H.; Gross, R.; Bushman, F. D.; Collman, R. G.; Liu, C. Miniaturized Devices for Point of Care Molecular Detection of HIV. *Lab Chip* **2017**, *17* (3), 382–394.
(20) Notomi, T. Loop-Mediated Isothermal Amplification of DNA. *Nucleic Acids Research* **2000**, *28* (12), 63e–663. https://doi.org/10.1093/nar/28.12.e63.
(21) Mori, Y.; Nagamine, K.; Tomita, N.; Notomi, T. Detection of Loop-Mediated Isothermal Amplification Reaction by Turbidity Derived from Magnesium Pyrophosphate Formation. *Biochemical and Biophysical Research Communications* **2001**, *289* (1), 150–154. https://doi.org/10.1006/bbrc.2001.5921.
(22) Nagamine, K.; Watanabe, K.; Ohtsuka, K.; Hase, T.; Notomi, T. Loop-Mediated Isothermal Amplification Reaction Using a Nondenatured Template. *Clinical Chemistry* **2001**, *47* (9), 1742–1743. https://doi.org/10.1093/clinchem/47.9.1742.
(23) Parida, M.; Horioke, K.; Ishida, H.; Dash, P. K.; Saxena, P.; Jana, A. M.; Islam, M. A.; Inoue, S.; Hosaka, N.; Morita, K. Rapid Detection and Differentiation of Dengue Virus Serotypes by a Real-Time Reverse Transcription-Loop-Mediated Isothermal Amplification Assay. *J Clin Microbiol* **2005**, *43* (6), 2895–2903. https://doi.org/10.1128/JCM.43.6.2895-2903.2005.
(24) Tomita, N.; Mori, Y.; Kanda, H.; Notomi, T. Loop-Mediated Isothermal Amplification (LAMP) of Gene Sequences and Simple Visual Detection of Products. *Nature protocols* **2008**, *3* (5), 877.
(25) Parida, M.; Sannarangaiah, S.; Dash, P. K.; Rao, P. V. L.; Morita, K. Loop Mediated Isothermal Amplification (LAMP): A New Generation of Innovative Gene Amplification Technique; Perspectives in Clinical Diagnosis of Infectious Diseases. *Rev. Med. Virol.* **2008**, *18* (6), 407–421. https://doi.org/10.1002/rmv.593.
(26) Curtis, K. A.; Rudolph, D. L.; Morrison, D.; Guelig, D.; Diesburg, S.; McAdams, D.; Burton,

R. A.; LaBarre, P.; Owen, M. Single-Use, Electricity-Free Amplification Device for Detection of HIV-1. *J Virol Methods* **2016**, *237*, 132–137. https://doi.org/10.1016/j.jviromet.2016.09.007.

(27) Safavieh, M.; Kanakasabapathy, M. K.; Tarlan, F.; Ahmed, M. U.; Zourob, M.; Asghar, W.; Shafiee, H. Emerging Loop-Mediated Isothermal Amplification-Based Microchip and Microdevice Technologies for Nucleic Acid Detection. *Acs Biomater-Sci Eng* **2016**, *2* (3), 278–294. https://doi.org/10.1021/acsbiomaterials.5b00449.

(28) Phillips, E. A.; Moehling, T. J.; Bhadra, S.; Ellington, A. D.; Linnes, J. C. Strand Displacement Probes Combined with Isothermal Nucleic Acid Amplification for Instrument-Free Detection from Complex Samples. *Anal Chem* **2018**, *90* (11), 6580–6586. https://doi.org/10.1021/acs.analchem.8b00269.

(29) Choi, G.; Prince, T.; Miao, J.; Cui, L. W.; Guan, W. H. Sample-to-Answer Palm-Sized Nucleic Acid Testing Device towards Low-Cost Malaria Mass Screening. *Biosensors & bioelectronics* **2018**, *115*, 83–90. https://doi.org/10.1016/j.bios.2018.05.019.

(30) Choi, G.; Song, D.; Shrestha, S.; Miao, J.; Cui, L.; Guan, W. A Field-Deployable Mobile Molecular Diagnostic System for Malaria at the Point of Need. *Lab Chip* **2016**, *16* (22), 4341–4349. https://doi.org/10.1039/c6lc01078d.

(31) Liu, C.; Geva, E.; Mauk, M.; Qiu, X.; Abrams, W. R.; Malamud, D.; Curtis, K.; Owen, S. M.; Bau, H. H. An Isothermal Amplification Reactor with an Integrated Isolation Membrane for Point-of-Care Detection of Infectious Diseases. *The Analyst* **2011**, *136* (10), 2069–2076.

(32) Damhorst, G. L.; Duarte-Guevara, C.; Chen, W.; Ghonge, T.; Cunningham, B. T.; Bashir, R. Smartphone-Imaged HIV-1 Reverse-Transcription Loop-Mediated Isothermal Amplification (RT-LAMP) on a Chip from Whole Blood. *Engineering* **2015**, *1* (3), 324–335. https://doi.org/10.15302/J-ENG-2015072.

(33) Liu, T.; Choi, G.; Tang, Z.; Kshirsagar, A.; Politza, A. J.; Guan, W. Fingerpick Blood-Based Nucleic Acid Testing on A USB Interfaced Device towards HIV Self-Testing. *Biosensors and Bioelectronics*, 2022, *209*, 114255.

(34) Liao, S. C.; Peng, J.; Mauk, M. G.; Awasthi, S.; Song, J.; Friedman, H.; Bau, H. H.; Liu, C. Smart Cup: A Minimally-Instrumented, Smartphone-Based Point-of-Care Molecular Diagnostic Device. *Sens Actuators B Chem* **2016**, *229*, 232–238. https://doi.org/10.1016/j.snb.2016.01.073.

(35) Tang, Z. F.; Cui, J. R.; Kshirsagar, A.; Liu, T. Y.; Yon, M.; Kuchipudi, S. V.; Guan, W. H. SLIDE: Saliva-Based SARS-CoV-2 Self-Testing with RT-LAMP in a Mobile Device. *ACS sensors* **2022**. https://doi.org/10.1021/acssensors.2c01023.

(36) Choi, G.; Guan, W. Sample-to-Answer Microfluidic Nucleic Acid Testing (NAT) on Lab-on-a-Disc for Malaria Detection at Point of Need. In *Biomedical Engineering Technologies*; Ossandon, M. R., Baker, H., Rasooly, A., Eds.; Methods in Molecular Biology; Springer US: New York, NY, 2022; Vol. 2393, pp 297–313. https://doi.org/10.1007/978-1-0716-1803-5_16.

(37) Choi, G.; Guan, W. An Ultracompact Real-Time Fluorescence Loop-Mediated Isothermal Amplification (LAMP) Analyzer. In *Biomedical Engineering Technologies*; Ossandon, M. R., Baker, H., Rasooly, A., Eds.; Methods in Molecular Biology; Springer US: New York, NY, 2022; Vol. 2393, pp 257–278. https://doi.org/10.1007/978-1-0716-1803-5_14.

(38) Phillips, E. A.; Moehling, T. J.; Ejendal, K. F. K.; Hoilett, O. S.; Byers, K. M.; Basing, L. A.; Jankowski, L. A.; Bennett, J. B.; Lin, L. K.; Stanciu, L. A.; Linnes, J. C. Microfluidic Rapid and Autonomous Analytical Device (MicroRAAD) to Detect HIV from Whole Blood

Samples. *Lab Chip* **2019**, *19* (20), 3375–3386. https://doi.org/10.1039/c9lc00506d.
(39) Curtis, K. A.; Rudolph, D. L.; Nejad, I.; Singleton, J.; Beddoe, A.; Weigl, B.; LaBarre, P.; Owen, S. M. Isothermal Amplification Using a Chemical Heating Device for Point-of-Care Detection of HIV-1. *PloS one* **2012**, *7* (2), e31432. https://doi.org/10.1371/journal.pone.0031432.
(40) Chen, H.-W.; Ching, W.-M. Evaluation of the Stability of Lyophilized Loop-Mediated Isothermal Amplification Reagents for the Detection of Coxiella Burnetii. *Heliyon* **2017**, *3* (10), e00415. https://doi.org/10.1016/j.heliyon.2017.e00415.
(41) Vemulapati, S.; Erickson, D. Portable Resource-Independent Blood–Plasma Separator. *Anal. Chem.* **2019**, *91* (23), 14824–14828. https://doi.org/10.1021/acs.analchem.9b04180.
(42) Zhang, H.; Anoop, K.; Huang, C.; Sadr, R.; Gupte, R.; Dai, J.; Han, A. A Circular Gradient-Width Crossflow Microfluidic Platform for High-Efficiency Blood Plasma Separation. *Sensors and Actuators B: Chemical* **2022**, *354*, 131180. https://doi.org/10.1016/j.snb.2021.131180.
(43) Liu, C.; Liao, S.-C.; Song, J.; Mauk, M. G.; Li, X.; Wu, G.; Ge, D.; Greenberg, R. M.; Yang, S.; Bau, H. H. A High-Efficiency Superhydrophobic Plasma Separator. *Lab Chip* **2016**, *16* (3), 553–560. https://doi.org/10.1039/C5LC01235J.
(44) Nabatiyan, A.; Parpia, Z. A.; Elghanian, R.; Kelso, D. M. Membrane-Based Plasma Collection Device for Point-of-Care Diagnosis of HIV. *Journal of Virological Methods* **2011**, *173* (1), 37–42. https://doi.org/10.1016/j.jviromet.2011.01.003.
(45) Baillargeon, K. R.; Murray, L. P.; Deraney, R. N.; Mace, C. R. High-Yielding Separation and Collection of Plasma from Whole Blood Using Passive Filtration. *Anal. Chem.* **2020**, *92* (24), 16245–16252. https://doi.org/10.1021/acs.analchem.0c04127.
(46) Kadimisetty, K.; Yin, K.; Roche, A. M.; Yi, Y.; Bushman, F. D.; Collman, R. G.; Gross, R.; Feng, L.; Liu, C. An Integrated Self-Powered 3D Printed Sample Concentrator for Highly Sensitive Molecular Detection of HIV in Whole Blood at the Point of Care. *Analyst* **2021**, *146* (10), 3234–3241. https://doi.org/10.1039/D0AN02482A.
(47) Robinson, M.; Marks, H.; Hinsdale, T.; Maitland, K.; Coté, G. Rapid Isolation of Blood Plasma Using a Cascaded Inertial Microfluidic Device. *Biomicrofluidics* **2017**, *11* (2), 024109. https://doi.org/10.1063/1.4979198.
(48) Guo, W.; Hansson, J.; Van Der Wijngaart, W. Synthetic Paper Separates Plasma from Whole Blood with Low Protein Loss. *Anal. Chem.* **2020**, *92* (9), 6194–6199. https://doi.org/10.1021/acs.analchem.0c01474.
(49) Liu, C.-H.; Chen, C.-A.; Chen, S.-J.; Tsai, T.-T.; Chu, C.-C.; Chang, C.-C.; Chen, C.-F. Blood Plasma Separation Using a Fidget-Spinner. *Anal. Chem.* **2019**, *91* (2), 1247–1253. https://doi.org/10.1021/acs.analchem.8b04860.
(50) Hauser, J.; Lenk, G.; Hansson, J.; Beck, O.; Stemme, G.; Roxhed, N. High-Yield Passive Plasma Filtration from Human Finger Prick Blood. *Anal. Chem.* **2018**, *90* (22), 13393–13399. https://doi.org/10.1021/acs.analchem.8b03175.
(51) Tan, W.; Zhang, L.; Doery, J. C. G.; Shen, W. Three-Dimensional Microfluidic Tape-Paper-Based Sensing Device for Blood Total Bilirubin Measurement in Jaundiced Neonates. *Lab Chip* **2020**, *20* (2), 394–404. https://doi.org/10.1039/C9LC00939F.
(52) Boom, R.; Sol, C. J.; Salimans, M. M.; Jansen, C. L.; Wertheim-van Dillen, P. M.; Van Der Noordaa, J. Rapid and Simple Method for Purification of Nucleic Acids. *J Clin Microbiol* **1990**, *28* (3), 495–503. https://doi.org/10.1128/jcm.28.3.495-503.1990.
(53) Hill-Ambroz, K. L.; Brown-Guedira, G. L.; Fellers, J. P. Modified Rapid DNA Extraction

Protocol for High Throughput Microsatellite Analysis in Wheat. *Crop Sci.* **2002**, *42* (6), 2088–2091. https://doi.org/10.2135/cropsci2002.2088.

(54) Aljanabi, S. Universal and Rapid Salt-Extraction of High Quality Genomic DNA for PCR-Based Techniques. *Nucleic Acids Research* **1997**, *25* (22), 4692–4693. https://doi.org/10.1093/nar/25.22.4692.

(55) Mogg, R. J.; Bond, J. M. A Cheap, Reliable and Rapid Method of Extracting High-Quality DNA from Plants. *Mol Ecol Notes* **2003**, *3* (4), 666–668. https://doi.org/10.1046/j.1471-8286.2003.00548.x.

(56) Saag, M. S.; Holodniy, M.; Kuritzkes, D. R.; O'Brien, W. A.; Coombs, R.; Poscher, M. E.; Jacobsen, D. M.; Shaw, G. M.; Richman, D. D.; Volberding, P. A. HIV Viral Load Markers in Clinical Practice. *Nat Med* **1996**, *2* (6), 625–629. https://doi.org/10.1038/nm0696-625.

(57) Ritchie, A. V.; Ushiro-Lumb, I.; Edemaga, D.; Joshi, H. A.; De Ruiter, A.; Szumilin, E.; Jendrulek, I.; McGuire, M.; Goel, N.; Sharma, P. I.; Allain, J.-P.; Lee, H. H. SAMBA HIV Semiquantitative Test, a New Point-of-Care Viral-Load-Monitoring Assay for Resource-Limited Settings. *J Clin Microbiol* **2014**, *52* (9), 3377–3383. https://doi.org/10.1128/JCM.00593-14.

(58) Palmer, S.; Wiegand, A. P.; Maldarelli, F.; Bazmi, H.; Mican, J. M.; Polis, M.; Dewar, R. L.; Planta, A.; Liu, S.; Metcalf, J. A. New Real-Time Reverse Transcriptase-Initiated PCR Assay with Single-Copy Sensitivity for Human Immunodeficiency Virus Type 1 RNA in Plasma. *Journal of clinical microbiology* **2003**, *41* (10), 4531–4536.

For TOC only